Journal of Hydrology 593 (2021) 125781

Contents lists available at ScienceDirect

Journal of Hydrology

journal homepage: www.elsevier.com/locate/jhydrol

Research papers

Estimating seasonal water budgets in global lakes by using multi-source remote sensing measurements

Tan Chen [a], Chunqiao Song [a,*], Linghong Ke [b,c], Jida Wang [d], Kai Liu [a], Qianhan Wu [a,e]

[a] Key Laboratory of Watershed Geographic Sciences, Nanjing Institute of Geography and Limnology, Chinese Academy of Sciences, Nanjing 210008, China
[b] State Key Laboratory of Hydrology-Water Resources and Hydraulic Engineering, Hohai University, Nanjing 210098, China
[c] College of Hydrology and Water Resources, Hohai University, Nanjing 211100, China
[d] Department of Geography and Geospatial Sciences, Kansas State University, Manhattan, KS 66506, USA
[e] Department of Earth Sciences, The University of Hong Kong, Hong Kong, China

ARTICLE INFO

This manuscript was handled by A. Bardossy, Editor-in-Chief, with the assistance of Purna Chandra Nayak, Associate Editor

Keywords:
Seasonality
Lake water storage
Reservoir
Satellite altimetry
Water cycle
Landsat

ABSTRACT

The seasonal change in lake water storage (LWSsc) reflect periodic fluctuations of the basin-scale water balance. However, the role of LWSsc in regulating the water budget at the global scale has not yet been investigated based on straight-forward observations. Quantifying LWSsc is necessary, especially under the context of global change. Available in-situ measurements of lake water levels and volumes are still scarce. Therefore, the Global Surface Water datasets of Joint Research Centre and multi-source satellite altimetry datasets through mathematical statistics methods are used in this study to address this issue. We estimate the LWSsc of 463 lakes and reservoirs worldwide with areas greater than 10 km^2, which represent nearly 64% of the total global lake area and 93% of the total lake volume capacity. Results show that the global seasonal water storage variation of these examined water bodies is 1390.91 ± 78.91 km^3, comprising 869.44 ± 67.35 km^3 from lakes and 521.46 ± 41.11 km^3 from reservoirs. The relatively large estimates of LWSsc are concentrated in North American and African basins. Among the watersheds, the seasonal fluctuations of lakes in the North American Lawrence basin make up the most substantial magnitude of 10.76% of the global LWSsc. The latitudinal direction zonality of LWSsc is relatively significant. The LWSsc is concentrated between 30° N and 60° N in the northern hemisphere and between the equator and 30° S in the southern hemisphere. Considering the geographic similarity and climatological zonality, the global LWSsc estimates are also extrapolated to other lakes without direct satellite altimetry observations on the basis of the average rate of the examined lakes distributed in the same Köppen – Geiger Climate Classification zones. The LWSsc is calculated with a consequence of 488.23 ± 14.72 km^3 for these extrapolated lakes, indicating an estimate of 1357.67 ± 68.94 km^3 for the LWSsc of the global natural lakes (>10 km^2). This initial estimation of LWSsc at a global scale will greatly help the improvement of our understanding of the seasonal behavior of lakes and reservoirs in regulating global and regional water cycles and the contribution of terrestrial water storage to sea level rise.

1. Introduction

Lakes are regarded as one of the most significant stores of terrestrial surface liquid water and play a crucial role in regulating regional climate, balancing ecosystems, and protecting biodiversity. The lake water resources are also widely utilized in different human-related activities, such as water conservation, hydropower, irrigation, and cultivation (Johnston et al., 2011; Wada et al., 2014; Zarfl et al., 2015). In the past decades, lakes in different regions have undergone various degrees of change because of global change (Williamson et al., 2009; Zhang et al., 2011; Sterling et al., 2013). Global warming or the rapid increase in surface temperatures has accelerated the melting of polar ice caps and the sea ice around them; this phenomenon has also increased the humidity, which brings more precipitation and further increases the unevenness of the distribution of lake water storage (Wang et al., 2018; Erler et al., 2019). Consequently, changes in lakes and reservoirs are increasingly concerned and all of their morphodynamic characteristics (e.g., water area, water level, and water storage) are particularly observed in changing environments (Crétaux et al., 2016). The current situation and variation trend of lake water storage is the basis for the

* Corresponding author.
E-mail address: cqsong@niglas.ac.cn (C. Song).

https://doi.org/10.1016/j.jhydrol.2020.125781
Received 18 September 2020; Accepted 17 November 2020
Available online 28 November 2020

estimation of the terrestrial water availability and becomes a particular subject for assessments of present and future water resources. As a result, the lake water storage change plays an important role in the global hydrological cycle and influences the hydrologic process (Hirschi et al., 2006; Yeh and Famiglietti, 2008).

Seasonal change in lake water storage (LWSsc) is an essential element in the global or regional water budget. It reflects the seasonal fluctuation of hydrological regime of lakes. Although lake water storage change in typical basins (Hirschi et al., 2006; Sheffield et al., 2009; Pan et al., 2012; Ehalt Macedo et al., 2019; Hamlington et al., 2019; Borja et al., 2020) or seasonal fluctuation of typical lakes and reservoirs (Gronewold and Stow, 2014; Zhou et al., 2016; Borja et al., 2020) has been studied previously, the seasonal change of water storage in lakes and reservoirs has not yet been measured directly at the global scale. At present, in-situ lake water storage measurements are sparse, especially in developing countries (Duan and Bastiaanssen, 2013). Since heterogeneous in situ networks are always poorly shared at global level (Biancamaria et al., 2016), the global LWSsc has been difficult to estimate and has not been known. As a result, the role of LWSsc in modulating global water cycles and the contribution to sea-level rise has been challenging to estimate.

Remote sensing provides an effective and straight-forward way of monitoring lakes and reservoirs in the macroscale area and has gained much attention in recent years. Studies on water extent monitoring have been conducted using different optical sensors and analyses of lake changes in interannual and decadal timescales (Du et al., 2014; Pekel et al., 2014; Yao et al., 2015; Feng et al., 2016; Sheng et al., 2016; Khandelwal et al., 2017; Yang et al., 2017; Zhu et al., 2020). Numerous studies have shown the possibility of observing water surface elevation on the basis of satellite altimetry by using different altimeter missions (Birkett, 1995; Frappart et al., 2006; Da Silva et al., 2010; Schwatke et al., 2015a; Villadsen et al., 2015; Zawadzki and Ablain, 2016; Zhang et al., 2019). To measure long-term lake water level at the global scale, recent studies have proposed altimetry datasets, such as the Hydroweb database established by Laboratoire d'Etudes en Géophysique et Océanographie Spatiales (LEGOS, Laboratory of Studies in Space Geophysics and Oceanography) (Crétaux et al., 2011), Database for Hydrological Time Series of Inland Waters (DAHITI) (Schwatke et al., 2015b), and the US Department of Agriculture (USDA) Global Reservoir and Lake Monitoring (G-REALM) datasets (Birkett et al., 2011). Consequently, analyzing the lake water storage variations becomes possible through these combinations of multi-satellite data and optical remote sensing images. Furthermore, the changes in lake water storage could be estimated based on the time series of water area and water level changes (Lu et al., 2013; Zheng et al., 2016; Avisse et al., 2017; Yao et al., 2019). Thus, estimating the global LWSsc based on multi-source measurements is feasible and necessary to reveal the magnitude of the seasonal water cycle in the global water budget, making the LWSsc spatially and temporally comprehensive.

Monitoring lakes and reservoirs about their morphodynamic characteristics using remote sensing have been approached mentioned above. However, the straight-forward estimation of the global LWSsc using remote sensing or geospatial data sets has yet been done. Our objective is to employ a simple and effective method to estimate the seasonal change in lake water storage at a global scale from satellite observations. Here, we quantify the LWSsc with uncertainty estimates of global lakes and reservoirs based on the Global Surface Water (GSW) datasets of the Joint Research Centre (JRC) and all available altimetry level time series from Hydroweb, DAHITI, and G-REALM. We then extrapolate the LWSsc estimates to other lakes without direct satellite measurements based on the average seasonal water-level variation of the examined lakes within the same climatological zones according to the Köppen – Geiger Climate Classification (Kottek et al., 2006). We aim to advance existing understanding of the role of the seasonal behavior of lakes and reservoirs in regulating the global and regional water cycles and the contribution of terrestrial water storage to sea level rise.

2. Study area and data

2.1. Investigated lakes and reservoirs worldwide

In the study, a total of 463 lakes and reservoirs with long-term satellite altimetry measurements were selected to estimate the global LWSsc and investigate their spatial patterns (see Supplementary Information Table S1 for attribute information of lakes and reservoirs studied). Fig. 1 shows the locations of these lakes and reservoirs, with lake area size and distribution. These contained 283 natural lakes and 180 reservoirs located on every continent. All the 463 large and medium-sized global lakes (149 from North America, 136 from Asia, 74 from South America, 54 from Africa, 39 from Europe, 11 from Oceania) are over 10 km^2 in size. These lakes, with a total area of 1393.25 thousand km^2 and a total volume of 171 thousand km^3, represent nearly 64% of the global lake area and 93% of the total volume capacity. The information on these lakes was obtained from the HydroLAKES database (http://www.hydrosheds.org) (Messager et al., 2016).

2.2. Study data

2.2.1. Altimetry water level datasets

In this study, water level time series from three merged altimetry data platforms, namely, Hydroweb, DAHITI, and G-REALM databases were used as input data for the LWSsc estimation. Established by LEGOS, the Hydroweb database was a combination of Topex/Poseidon, Jason-1/-2/-3, ENVISAT, and GFO measurements (Crétaux et al., 2011). This database contained the time series of water level observations with a decimeter precision for 155 global lakes and reservoirs selected in this study. The DAHITI database was based on a widespread outlier rejection and a Kalman filter approach and incorporated with cross-calibrated multi-mission altimeter data from Topex/Poseidon, Jason-1/-2/-3, ENVISAT, ERS-1/-2, Cryosat-2, and SARAL/AltiKa (Schwatke et al., 2015a). The DAHITI database was reported to achieve more accurate height information with an RMSE as low as 4–5 cm for large lakes and several decimeters for smaller lakes than the other available altimeter databases (Busker et al., 2019). Operated by USDA, G-REALM database merged Topex/Poseidon, Jason-1/-2/-3, and ENVISAT missions with temporal resolutions varying from 10 to 35 days (Birkett et al., 2011). The 10-day G-REALM product, which contains sufficient temporally data, was selected in this study.

2.2.2. Lake and reservoir area data

This study used the Yearly Water Classification History data layer of the JRC GSW dataset (Pekel et al., 2016) to calculate the annual maximum, minimum, and average surface areas of lakes and reservoirs investigated. The JRC GSW dataset is a high-resolution stack of images that maps the spatial and temporal distributions of surface water over the last 35 years from 1984 to 2018. This dataset was produced based on the entire image archive of the Landsat 5, 7, and 8. It recorded the months and years of water-land cover, water changes, seasonality, and persistence at 30 m resolution (Pekel et al., 2016). The Yearly Water Classification History data set provided information on the seasonality of the water year to year over the world. We could distinguish seasonal water and permanent water of lake and reservoir area each year through the Yearly Water Classification History data.

3. Methods

3.1. Constructing water level time series of lakes

First, we generated monthly mean values by integrating all of the water level observations and then averaging all the measurements for each lake in each month. Second, we filtered the surface elevation data from a combination of satellite altimeters, which met the requirements of owning a time series of five consecutive years during 1992 to 2018

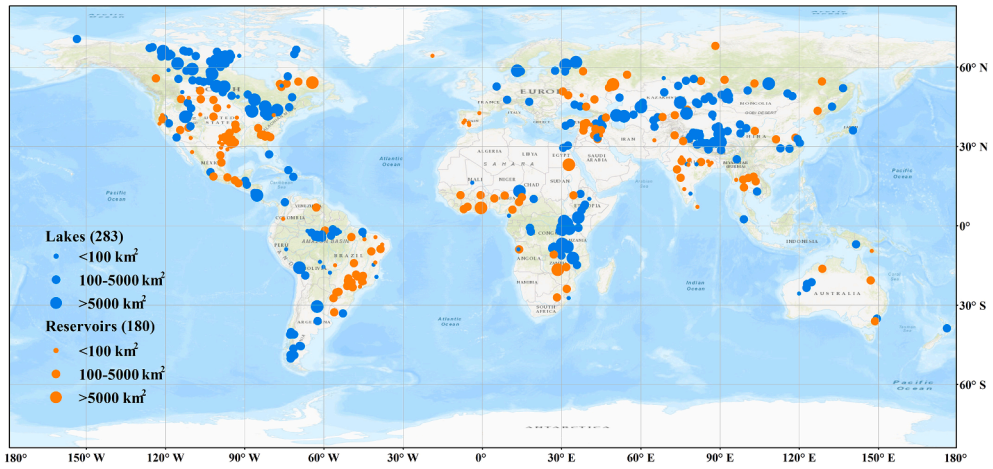

Fig. 1. Locations of the analyzed global lakes (blue) and reservoirs (orange). The background image shows the Esri World Topographic Map (http://goto.arcgisonline.com/maps/World_Topo_ Map). (For interpretation of the references to colour in this figure legend, the reader is referred to the web version of this article.)

and surface area larger than 10 km^2. Finally, we obtained the monthly water levels for all the study lakes and reservoirs.

Fig. 2 shows the number of observed lakes with a different number of observation years of water level. A total of 92 lakes had complete altimetry time series during the study period (1992–2018), accounting for nearly 20% of the total number of studied lakes. The time series of altimetry water levels for most of the study lakes (92.7%) have a temporal coverage of 9 years, whereas only 34 lakes had been observed for less than 9 years. The median of the observed period was 13 years for the examined lakes.

3.2. Retrieval of annual average inundation area of lakes

We used the Yearly Water Classification History dataset, a set of maps in a raster format showing annual global water-land cover with surface water changes from 1984 to 2018. We examined the inundation areas of lakes and reservoirs from the 27 years dataset from 1992 to 2018, considering the time range of altimetry water level data. We classified four categories in the dataset: permanent water, seasonal water, land, and no observations (Fig. 3). We selected the seasonal and permanent water categories to calculate the annual average maximum (seasonal and permanent water pixels) and minimum (permanent water pixels) areas of each lake or reservoir on the Google Earth Engine platform. We then obtained the multi-year averaged maximum and minimum lake areas by averaging the maximum and minimum lake areas recorded within the study periods. As an example of the retrieval of the annual average inundation area of lakes studied, we performed the sample and processing of the Aral Sea showed in Fig. 3.

3.3. Estimation of seasonal water storage and uncertainty

In general, the bottom morphology of lakes and reservoirs was assumed to be regular with a pyramidal shape (Abileah et al., 2011). Therefore, the seasonal water storage variations (ΔV_i) can be derived from the following equation (Taube, 2000):

$$\Delta h_{ij} = \frac{1}{n}\sum_{i}^{n}\left(h_{ijmax} - h_{ijmin}\right) \quad (1)$$

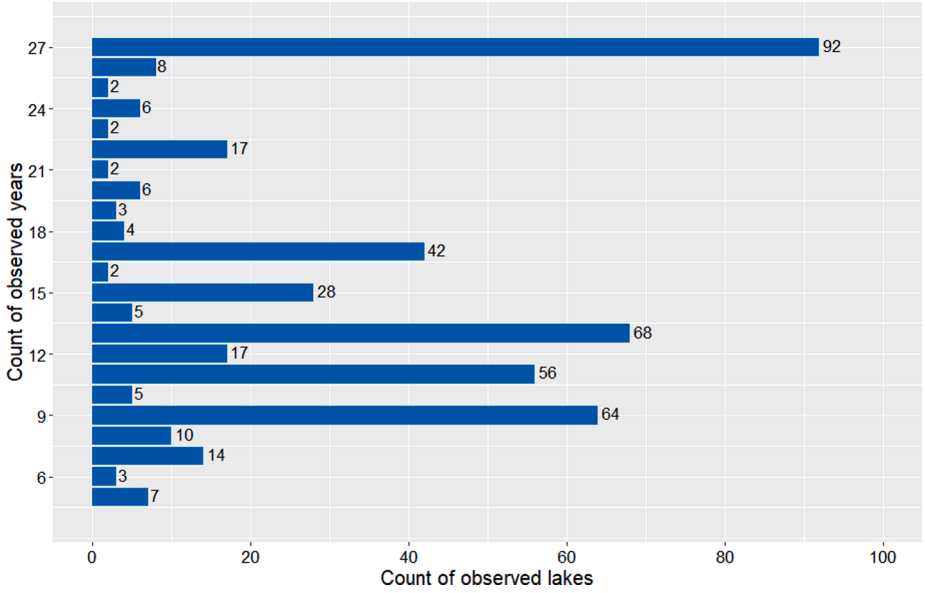

Fig. 2. Frequency of observed years used to estimate the LWSsc for the 483 analyzed lakes and reservoirs, with the total number of observations for lakes in different continuous time series categories.

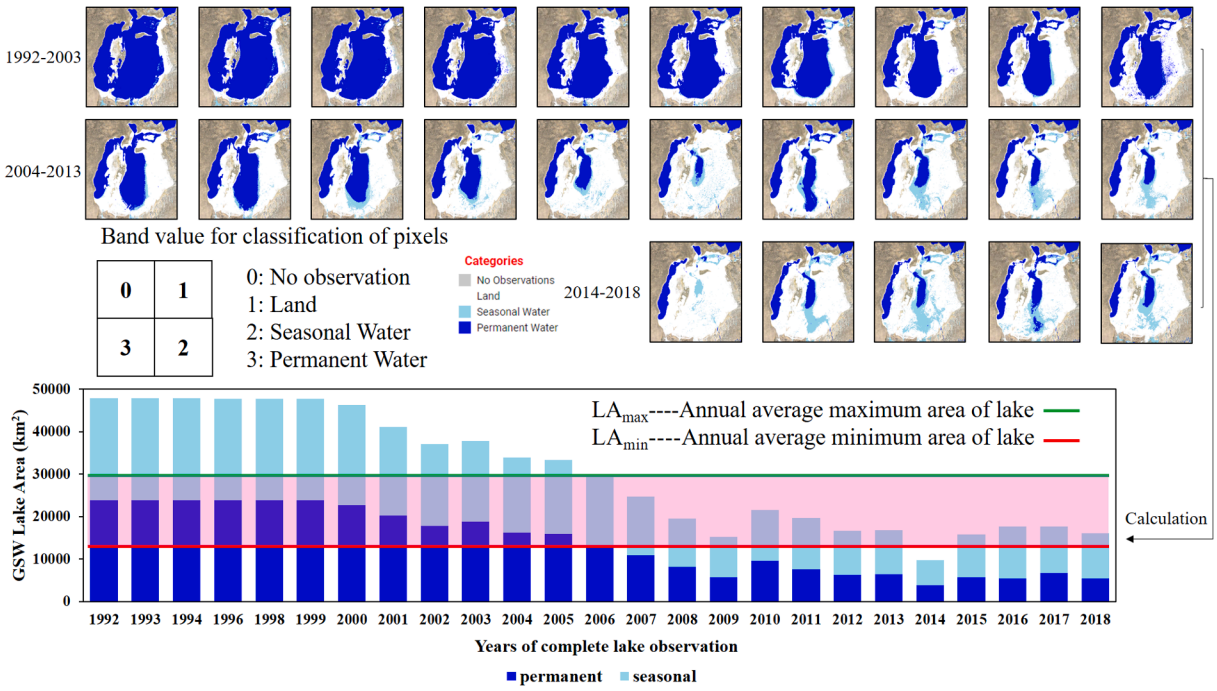

Fig. 3. GSW Yearly Water Classification History dataset sample and area calculation. Example of the Aral Sea in Central Eurasia. In the top panel, time-series water–land classification maps show the seasonal and permanent water inundation area on the basis of GSW datasets. In the bottom panel, the calculation process of the multi-year average min and max lake areas is shown. The green line is the multi-year average max lake area of Aral Sea marked as LA_{max}, whereas the red line is multi-year average min lake area of Aral Sea marked as LA_{min}. The pink stripe means the average seasonal fluctuation inundation range of the Aral Sea from 1992 to 2018. (For interpretation of the references to colour in this figure legend, the reader is referred to the web version of this article.)

$$\Delta V_j = \Delta h_{ij} \times \frac{\left(\overline{A}_{ijmax} + \overline{A}_{ijmin} + \sqrt{\overline{A}_{ijmax}} \times \overline{A}_{ijmin}\right)}{3} \quad (2)$$

where Δh_{ij} is the multi-year mean seasonal water level change (defined as $h$max – $h$min in the year *i of lake j*, reflected the intra-annual level range), $h_{ijmax}$is the maximum water level, and h_{ijmin} is the minimum water level from altimetry for the year i of lake j. $\overline{A}_{jmax}$and $\overline{A}_{jmin}$ are the multi-year mean calculated maximum and minimum lake areas derived from the GSW dataset. ΔV_j is the seasonal water storage variations of the lake j.

Moreover, the uncertainty of estimation is calculated considering the changes in surface water level, the average maximum area, and the minimum area of study lakes by using Eq. (3).

$$\Delta V_{STD} = \sqrt{\left(\Delta h^2 \times \left(A^2_{max\_STD} + A^2_{min\_STD}\right) + \Delta h^2_{STD} \times \left(\overline{A}^2_{max} + \overline{A}^2_{min}\right)\right)} \quad (3)$$

When calculated the aggregated uncertainties, we employed the error propagation law showed like the Eq. (4).

$$\Delta V_{STD\_sum} = \sqrt{\Delta V^2_{STD1} + \Delta V^2_{STD2} + \ldots + \Delta V^2_{STDj-1} + \Delta V^2_{STDj}} \quad (4)$$

where ΔV_{STD} is the standard deviation of estimated LWSsc, defined as the uncertainty of each lake. Δh is the multi-year mean seasonal water level change, and Δh_{STD} is the mean standard deviation of multi-year Δh. $\overline{A}_{max}$and $\overline{A}_{min}$ are the multi-year mean calculated maximum and minimum lake areas derived from the GSW dataset. A_{max_STD} and A_{min_STD} are the standard deviations of maximum and minimum lake areas in different years. ΔV_{STD_sum} is the aggregated uncertainties based on error propagation law by the Eq. (4).

4. Results

4.1. Analyses of LWSsc estimates by continent

The LWSsc of 463 water bodies (lakes and reservoirs, >10 km^2) located in different continents are estimated. Table 1 provides the summary of the water level changes (△H), the maximum water surface area, the minimum water surface area, and the LWSsc (△V) with standard deviations (STDs) of the target lakes and reservoirs per continent. The majority of the studied lakes are located in Asia and North America, which make up more than 60% (quantity: 285, proportion: 62%), while the smallest target number of lakes (11) in Oceania (a majority of them belong to Australia). Globally, the LWSsc of studied water bodies is 1390.91 ± 78.91 km^3. The North American lakes show the highest seasonal fluctuation of water storage of 435.18 ± 42.08 km^3, given that most lakes in this continent have large surface areas. Europe has an LWSsc of approximately 311.64 ± 48.68 km^3, owing to the super-large lake Caspian Sea (assigned to Europe when categorizedby continents). The lakes in Europe lead in terms of maximum and minimum water surface area of 462.4 ± 12.77 thousand km^2 and 459.2 ± 11.75 thousand km^2, respectively. The lakes in South America (186 ± 28.01 km^3) and Africa (250.15 ± 29.19 km^3) show high variability in water surface level with 4.54 ± 1.45 m and 3.86 ± 1.63 m, respectively, suggesting their complex topography and highly hydro-climatological dynamic variations. However, the causes of seasonal fluctuations in the lakes in these two continents are not entirely identical. The vast lake inundation areas have dominated the LWSsc of the African water bodies. Frequent flooding of the major river lagoons and reservoirs in South America dominates the seasonal fluctuations accompanied by the variations in water level.

Table 1
Summary of the average seasonal water storage of the 463 water bodies by continent.

Continent	Number of water bodies	△H (m)		Max Area (thousand km^2)		Min Area (thousand km^2)		△V (km^3)	
		Mean	STD	Total	STD	Total	STD	Total	STD
Africa	54	3.86	1.63	198.66	2.44	193.29	2.20	250.15	29.19
Asia	136	3.71	1.41	144.44	9.17	136.26	11.44	201.53	21.15
Europe	39	2.88	1.10	462.40	12.77	459.20	11.75	311.64	48.68
North America (N.A.)	149	2.94	1.29	445.89	2.68	442.88	3.05	435.18	42.08
South America (S.A.)	74	4.54	1.45	69.02	2.21	64.09	3.49	186.00	28.01
Oceania	11	2.84	1.33	3.27	0.18	2.12	0.16	6.41	1.43
Global	463	3.52	1.38	1323.67	29.45	1297.84	32.09	1390.91	78.91

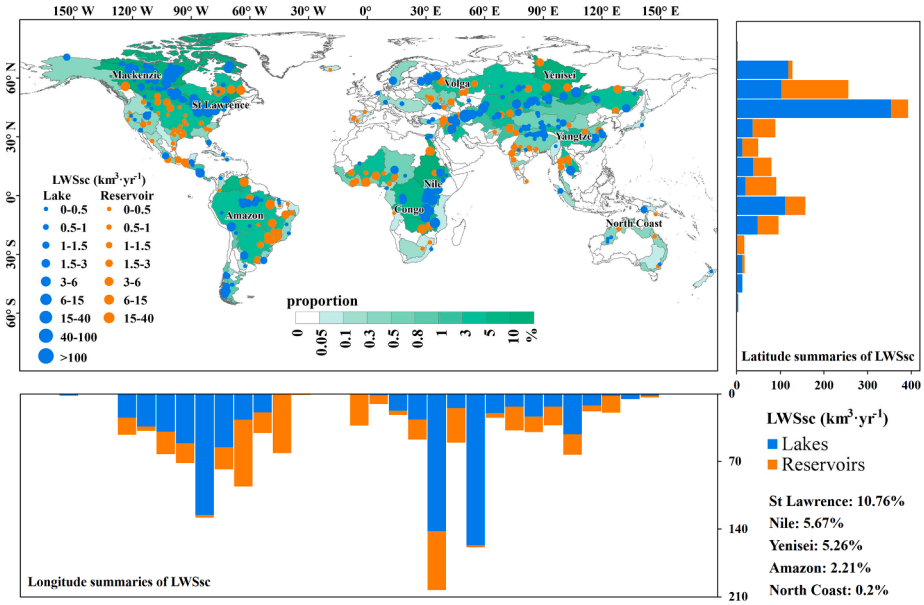

Fig. 4. Global lakes and reservoirs average LWSsc and distribution in the major basins. Global maps with 10° latitude/longitude summaries of average LWSsc are shown on the right and underneath. The global map shows lakes (blue dots), reservoirs (orange dots), and LWSsc magnitude (dot radius) located in different watersheds. Green global map background with colormap rendering represents the proportion of the LWSsc. (For interpretation of the references to colour in this figure legend, the reader is referred to the web version of this article.)

4.2. Analyses of the spatial characteristic of the LWSsc of global lakes and reservoirs

Fig. 4 shows the spatial distribution map of the LWSsc estimates of different water bodies. The LWSsc are calculated with 10° latitude/longitude summaries on the right and underneath panels of the global map (Fig. 4). Globally, the study lakes and reservoirs show significant seasonal fluctuations. The total LWSsc of examined lakes and reservoirs are 869.44 ± 67.35 and 521.46 ± 41.11 km^3, respectively. Considerable LWSsc are distributed in the North American lakes, the South American large reservoirs, the Eurasian lakes, and the Africa Great Rift Valley lakes. The Caspian Sea of Eurasia exhibits a significant seasonal fluctuation with the largest LWSsc (144.85 ± 44.98 km^3). The second-largest LWSsc are observed for the Great Rift Valley Lakes in Africa and the Great Lakes in North America (including Malawi Lake, Victoria Lake, Lake Superior, Lake Michigan, and Lake Huron). The seasonal fluctuation of each lake is between 27 ± 14.11 to 31 ± 6.71 km^3. Furthermore, the study reservoirs also have large LWSsc. Guri Reservoir (37.78 ± 24.84 km^3) in South America has led the largest LWSsc among the analyzed reservoirs. Tucurui Reservoir (South America), Lake Nasser (Africa), and Lake Volta (Africa) have relatively high seasonal fluctuations over 20 km^3 compared withother study reservoirs.

The latitudinal direction zonality of LWSsc can be clearly observed in Fig. 4. The LWSsc is mainly distributed in the middle and high latitudes of the northern hemisphere. A secondary LWSsc peak distributed in the low latitudes is also observed around the equator. The LWSsc is less obvious in the middle and high latitudes of the southern hemisphere due to fewer observed lakes in this area. Among the investigated basins, the higher magnitudes of LWSsc are distributed in the Mackenzie basin (North America), the Saint Lawrence basin (North America), the Amazon basin (South America), the Nile basin (Africa), the Caspian Sea (Eurasia), and the Yenisei basin (Eurasia). The studied lakes in the Saint Lawrence basin, where the North American Great Lakes are located, make up the largest proportion of nearly 11% (10.76%) of the global LWSsc. In summary, the amount of LWSsc is more concentrated between 30° N and 60° N of the northern hemisphere. The amount of LWSsc is focused between the equator and 30° S of southern hemisphere.

4.3. Analyses of long-term LWSsc estimates based on typical lakes

To further reveal the change in the characteristics of LWSsc throughout the study period, we select five lakes and reservoirs located in different basins with considerable seasonal fluctuations and long-term satellite altimetry measurements as examples to demonstrate the annual LWSsc time series, as shown in Fig. 5. The estimated LWSsc of the study lakes is between the maximum and the minimum annual LWSsc. The Caspian Sea, with a surface area of 0.38 million km^2, is the largest lake in the world (Mehdinia et al., 2020). This lake has exhibited a fluctuating pattern, displaying the seasonally fluctuating increase in the water storage during 1992 to 2018 (Fig. 5c). This lake's estimated LWSsc of 144.85 ± 44.98 km^3 is between the lower annual LWSsc of 21.41 ± 11.41 km^3 and the upper annual LWSsc of 227.54 ± 89.29 km^3 and close to the annual average LWSsc of 135.82 ± 62.01 km^3. Other estimated LWSsc of typical lakes also reflected the average level of interannual fluctuations, for example, Malawi Lake at 31.45 ± 14.57 km^3 (lower limit: 26.63 ± 11.01 km^3, upper limit: 38.14 ± 17.93 km^3), Superior Lake at 30.97 ± 16.32 km^3 (lower limit: 13.94 ± 6.87 km^3, upper limit: 57.38 ± 27.65 km^3), Guri Reservoir at 37.78 ± 24.84 km^3 (lower limit:

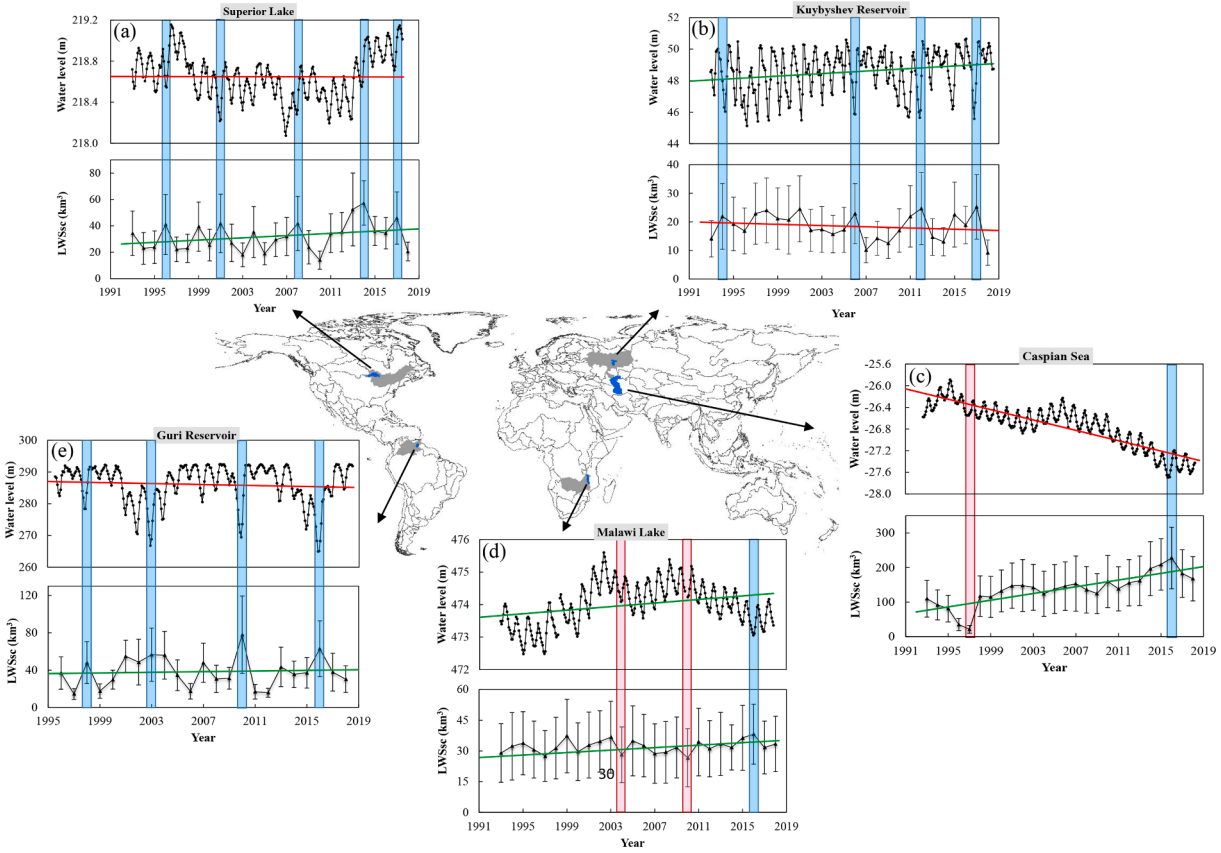

Fig. 5. Examples of LWSsc from the typical lake with affiliated basins: (a) Superior Lake (St. Lawrence basin, North America), (b) Kuybyshev Reservoir (Volga basin, Europe), (c) Caspian Sea (Eurasia), (d) Malawi Lake (Zambezi basin, Africa), and (e) Guri Reservoir (Orinoco basin, South America). The study lakes are shown with water level time series and trendline to understand further the temporal characteristics of the LWSsc. The red trendline means a linear decrease, whereas the green trend line means a linear increase. The red and blue stripes mark the synchronous feature between the time-series variation of LWSsc and water level (red stripe represents small LWSsc and changes in water level, whereas blue stripe represents large LWSsc and changes in water level). (For interpretation of the references to colour in this figure legend, the reader is referred to the web version of this article.)

14.41 ± 4.83 km^3, upper limit: 77.93 ± 41.45 km^3), and Kuybyshev Reservoir at 18.76 ± 6.29 km^3 (lower limit: 9.19 ± 4.39 km^3, upper limit: 25.23 ± 12.58 km^3).

Intuitively, the LWSsc is dependable on the seasonal changes of lake level. For example, the synchronous feature between the time-series variation of LWSsc and water level are marked as the red and blue stripes in Fig. 5. However, the interannual variations of the LWSsc do not always depend on the changing trend of water level in the long term. The pattern for these examined lakes can be divided into three categories. The first category includes Lake Superior, Guri Reservoir, and the Caspian Sea. As the water level decreases in these bodies of water, the LWSsc increases, especially for the Caspian Sea. The second category is represented by the Malawi Lake, whose water level and LWSsc are increasing synchronously. The third category includes the Kuybyshev Reservoir, which is characterized by decreasing LWSsc but rising water levels.

5. Discussion

5.1. Comparison among different LWSsc calculation methods

In this study, the seasonal amplitudes of lake water level were estimated by calculating the multi-year averaged differences between intra-annual maximum and minimum water levels. This process was termed as the LWSsc_Mean method. We applied here the Seasonal-Trend Decomposition Procedure Based on Loess (STL) method to decompose the time-series seasonal variations of water level and compare them with the performance of LWSsc estimation results used in this study. The STL was a statistical method of decomposing a time series data into four components containing data display, seasonality, trend, and residual. We employed the seasonal amplitudes to replace multi-year variations in water levels to calculate the LWSsc. This process was termed as the LWSsc_STL method. Then, we picked four lakes (i.e., Tanganyika Lake, Malawi Lake, Huron Lake, and Kuybyshev Reservoir) with diverse water level ranges and long-term satellite altimetry measurements to conduct a comparison among different LWSsc calculation methods. The two methods used to estimate the LWSsc and the annual time series of seasonal fluctuations of water storage are shown beneath the STL decomposition of water level for each lake in Fig. 6.

Generally, the estimates derived from the LWSsc_STL method were smaller than those obtained from the LWSsc_Mean method. The LWSsc_STL method decomposed the high-frequency noise signal and several years of periodic vibration trend. Although the LWSsc_Mean method could smooth seasonal fluctuations in the trend, it cannot eliminate high-frequency noises and periodic variations. However, the LWSsc of Tanganyika Lake (21.35 km^3), Malawi Lake (22.19 km^3), Huron Lake (20.73 km^3), and Kuybyshev Reservoir (14.03 km^3) calculated using the LWSsc_STL method were within the standard deviation range of estimates by the LWSsc_Mean method (e.g., Tanganyika lake, 24.67 ± 8.41 km^3; Malawi Lake, 31.45 ± 14.57 km^3; Huron lake, 27.86 ± 14.11 km^3; and Kuybyshev Reservoir, 18.76 ± 6.29 km^3). Moreover, the biases of the LWSsc exhibited by the LWSsc_Mean method for the sample lakes were within 30% compared with the result derived from the LWSsc_STL method. No complete and regular time series of water level was used because of the absence of satellite altimetry data in many lakes. Therefore, the LWSsc_Mean method can still be acceptable to

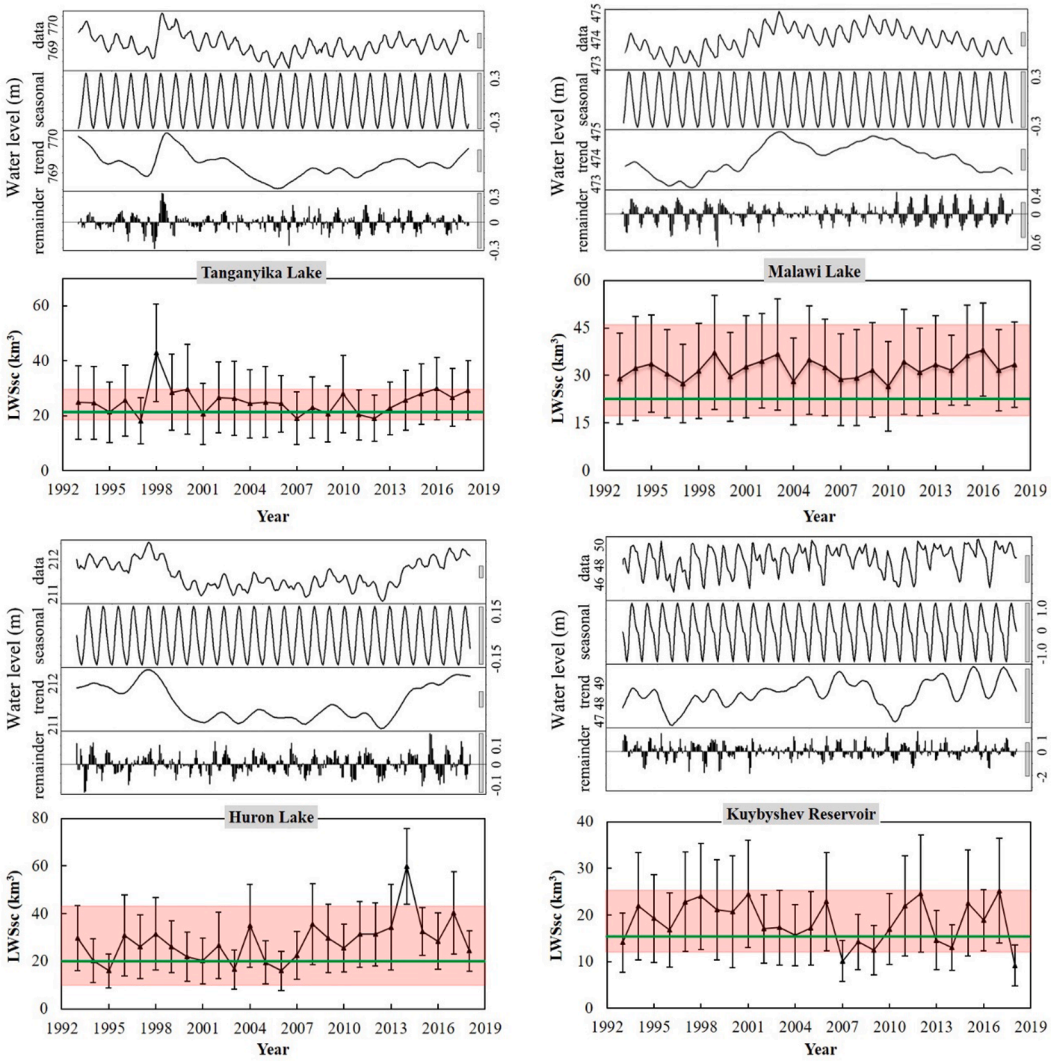

Fig. 6. Time series decomposition of monthly water elevation (satellite altimetry records), and time series of annual LWSsc for sample lakes. The red stripe represents the range of multi-year average estimated results of LWSsc for sample lakes. The green line represents the LWSsc based on the LWSsc_STL method. (For interpretation of the references to colour in this figure legend, the reader is referred to the web version of this article.)

estimate the LWSsc.

5.2. Estimation of the LWSsc of other global lakes without direct satellite measurements

Given that the satellite altimetry was limited to their footprint size, incomplete observations, and other reasons, we could not cover every lake, especially those with small surface areas. Considering the geographic similarity and the climate regulating effect of climatological zonality on lake water storage, we assumed that the lakes had relatively comparable seasonal fluctuations in the same climate zone. Accordingly, we employed the three-level classification system of Köppen – Geiger Climate Classification (Kottek et al., 2006) to estimate the LWSsc of 14,333 global lakes determined by the HydroLAKES database with surface areas above 10 km^2 without direct altimetry satellite measurements (see Fig. 7 for the climate area distribution). We excluded the reservoirs in this estimation because the water storage changes in this body of water were regulated by human operations. Then, we extrapolated the LWSsc of the unobserved lakes on the basis of geographically and lake-capacity weighted and provided a summary with the examined lakes by climate zone, as shown in Table 2. The maximum LWSsc was found with 515.12 ± 36.86 km^3 in the Df climate (Df for snow and fully humid, together with hot summer, warm summer, and cool summer). North American and Eurasian lake groups had the most LWSsc because of the abundance of lakes in the Df climate zone. The lakes in the Df climate, especially those with snow climate and fully humid with cool summer zone, exhibited the maximum LWSsc value of 300.83 ± 18.54 km^3. The minimum LWSsc amount of 1.13 ± 0.23 km^3 observed in the As climate zone (As for equatorial savannah with dry summer) was due to their limited number of lakes.

In summary, the total LWSsc of examined and extrapolated lakes were 869.44 ± 67.35 and 488.23 ± 14.72 km^3, respectively. The LWSsc of 283 observed lakes occupied a proportion of 64.04% compared with 1357.67 ± 68.94 km^3, which is the total occupied proportion of the lakes with surface areas above 10 km^2 worldwide. The number of lakes, whether examined or extrapolated in this study, occupied a similar proportion in each climate zone or continent. Therefore, the estimated LWSsc can be extended to global lakes as a significant reference. Currently, the number of lakes is of large uncertainty due to their global distribution (Verpoorter et al., 2014). This global estimate only considered lakes with the water mask above 10 km^2 from the HydroLAKES database. The global estimate methodology could be employed to future high-resolution measurements satellite missions, for instance, the Surface Water and Ocean Topography (SWOT) satellite mission, which goals to detect lakes with an area large 250 × 250 m^2 (Biancamaria et al., 2016).

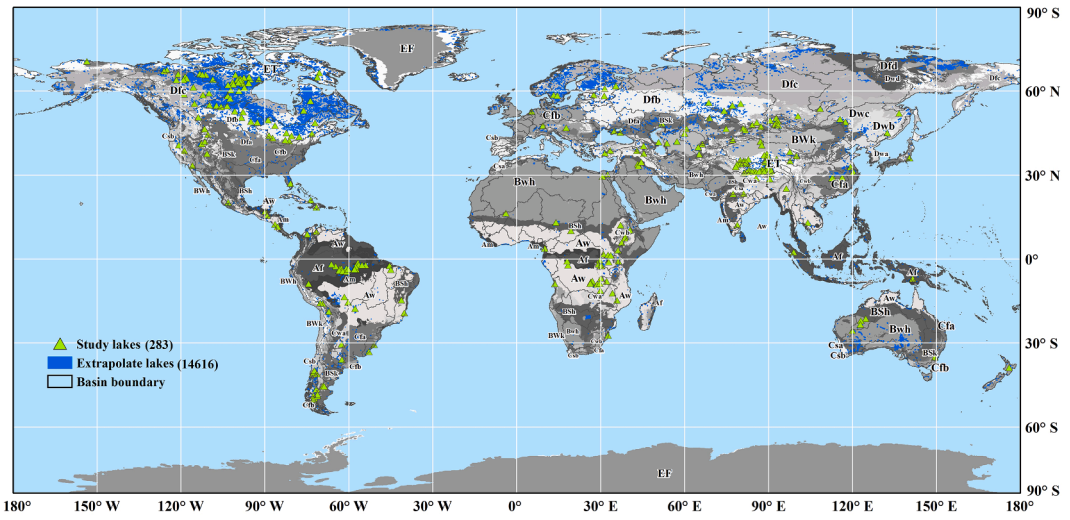

Fig. 7. Global distribution of study lakes (green triangle), extrapolate lakes (blue polygon), and world map of Köppen – Geiger Climate Classification (Main climates, A: equatorial, B: arid, C: warm temperate, D: snow, E: polar; Precipitation, W: desert, S: steppe, f: fully humid, s: summer dry, w: winter dry, m: monsoonal; Temperature, a: hot summer, b: warm summer, c: cool summer, d: extremely continental, h: hot arid, k: cold arid; F: polar frost; and T: polar tundra). (For interpretation of the references to colour in this figure legend, the reader is referred to the web version of this article.)

Table 2
Estimation of LWSsc for the lakes above 10 km^2 based on extrapolation compared to investigated lakes.

Climate	Examined lakes			Extrapolate lakes			Total lakes		
Classification	Count	△V (km^3)	STD (km^3)	Count	△V (km^3)	STD (km^3)	Count	△V (km^3)	STD (km^3)
Af	15	21.81	2.39	189	20.57	2.91	204	42.38	3.76
Am	9	9.66	1.68	200	36.95	2.59	209	46.61	3.09
As	1	0.29	0.06	25	0.84	0.22	26	1.13	0.23
Aw	39	164.02	22.24	566	1.42	0.11	605	165.44	22.24
BSh	6	1.48	1.25	183	8.89	0.99	189	10.37	1.59
BSk	27	38.26	7.81	477	0.36	0.05	504	38.62	7.81
BWh	11	21.64	7.97	316	24.99	6.97	327	46.62	10.59
BWk	22	43.94	14.38	229	2.16	0.69	251	46.1	14.40
Cfa	12	22.75	6.78	497	38.69	4.62	509	61.44	8.21
Cfb	10	8.11	2.46	438	13.58	1.31	448	21.69	2.78
Csa	6	8.11	2.45	89	2.75	0.53	95	10.86	2.50
Csb	4	3.96	1.17	83	3.04	0.67	87	7.01	1.35
Cwa	2	4.23	3.35	98	2.47	0.37	100	6.7	3.37
Cwb	2	7.34	1.88	29	0.48	0.06	31	7.82	1.88
Dfa	4	44.84	15.28	74	0.07	0.01	78	44.9	15.28
Dfb	28	155.24	27.95	2155	14.15	0.59	2183	169.39	27.96
Dfc	37	79.86	15.18	5907	220.96	10.64	5944	300.83	18.54
Dsc	6	26.88	16.03	708	7.42	0.66	714	34.3	16.05
Dwa	1	4.83	3.11	121	5.57	0.77	122	10.4	3.20
Dwc	9	33.75	7.71	88	2.09	0.29	97	35.84	7.71
ET	31	23.6	5.59	1861	80.77	3.57	1892	104.37	6.64
Caspian Sea	1	144.85	44.98				1	144.85	44.98
Total	283	869.44	67.35	14,333	488.23	14.72	14,616	1357.67	68.94

6. Conclusion

This study estimated the LWSsc for a total of 463 global lakes and reservoirs worldwide with inundation areas above 10 km^2 by combining the JRC GSW dataset with the satellite altimetry datasets, which represent nearly 64% of the global lake area and 93% of the total lake volume. The LWSsc of these examined water bodies was estimated at 1390.91 ± 78.91 km^3, including 869.44 ± 67.35 km^3 for natural lakes and 521.46 ± 41.11 km^3 for reservoirs. The zonality in latitudinal direction of LWSsc is relatively significant. The amount of LWSsc was more concentrated between 30° N and 60° N of the northern hemisphere. The larger LWSsc can be observed between the equator and 30° S of the southern hemisphere. LWSsc in North America Great Lakes made up the most substantial magnitude of nearly 11% (10.76%) of the seasonal water storage variations of the global lakes. The basins with relatively large seasonal lake water storage variations concentrated in North America and Africa had a significant seasonal fluctuation with more uncertainty. We also extrapolated a total of 14,616 global lakes (>10 km^2) with total LWSsc of 1357.67 ± 68.94 km^3 on the basis of the examined lakes within the similar climatological and hydrological zones.

The inadequate coverage of satellite altimetry measurements on lake water level, especially for the continents Oceania and Africa, was considered a limitation for the global LWSsc estimation in this study. Therefore, future studies are encouraged to develop different techniques to decrease the no-data percentage in lake observations. In the prospective study plan, recently launched or planned satellite altimetry missions, e.g., ICESat-2 and SWOT, and increasing altimetry water level databases will be a great help in improving the spatial coverage of lake water bodies and quantification accuracy of LWSsc.

CRediT authorship contribution statement

Tan Chen: Conceptualization, Data curation, Formal analysis, Investigation, Methodology, Resources, Software, Validation, Visualization, Writing - original draft, Writing - review & editing. **Chunqiao Song:** Conceptualization, Formal analysis, Funding acquisition, Methodology, Project administration, Resources, Supervision, Validation, Writing - original draft. **Linghong Ke:** Data curation, Investigation, Methodology, Resources, Software, Visualization, Writing - review & editing. **Jida Wang:** Formal analysis, Validation, Writing - review & editing. **Kai Liu:** Data curation, Funding acquisition, Software, Supervision, Writing - review & editing. **Qianhan Wu:** Data curation.

Declaration of Competing Interest

The authors declare that they have no known competing financial interests or personal relationships that could have appeared to influence the work reported in this paper.

Acknowledgments

This work was partly funded by the Strategic Priority Research Program of the Chinese Academy of Sciences (Grant No. XDA23100102), the National Key Research and Development Program of China (Grant Nos. 2018YFD0900804, 2019YFA0607101, and 2018YFD1100101), the Thousand Young Talents Program in China (Grant No. Y7QR011001), and the National Natural Science Foundation of China (No. 41971403).

Appendix A. Supplementary data

Supplementary data to this article can be found online at https://doi.org/10.1016/j.jhydrol.2020.125781.

References

Abileah, R., Vignudelli, S., Scozzari, A., 2011. A completely remote sensing approach to monitoring reservoirs water volume. Int. Water Technol. J 1, 63–77.
Avisse, N., Tilmant, A., Müller, M.F., Zhang, H., 2017. Monitoring small reservoirs' storage with satellite remote sensing in inaccessible areas. Hydrol. Earth Syst. Sci. 21 (12), 6445–6459.
Biancamaria, S., Lettenmaier, D.P., Pavelsky, T.M., 2016. The SWOT mission and its capabilities for land hydrology. Surveys Geophys. 37 (2), 307–337.
Birkett, C., 1995. The contribution of TOPEX/POSEIDON to the global monitoring of climatically sensitive lakes. J. Geophys. Res.: Oceans 100 (C12), 25179–25204.
Birkett, C., Reynolds, C., Beckley, B., Doorn, B., 2011. From research to operations: The USDA global reservoir and lake monitor. Coastal altimetry. Springer 19–50.
Borja, S., Kalantari, Z., Destouni, G., 2020. Global Wetting by Seasonal Surface Water Over the Last Decades. Earth's Future e2019EF001449.
Busker, T., et al., 2019. A global lake and reservoir volume analysis using a surface water dataset and satellite altimetry. Hydrol. Earth Syst. Sci. 23 (2), 669–690.
Crétaux, J.-F., et al., 2016. Lake volume monitoring from space. Surv. Geophys. 37 (2), 269–305.
Crétaux, J.-F., et al., 2011. SOLS: A lake database to monitor in the Near Real Time water level and storage variations from remote sensing data. Adv. Space Res. 47 (9), 1497–1507.
Da Silva, J.S., et al., 2010. Water levels in the Amazon basin derived from the ERS 2 and ENVISAT radar altimetry missions. Remote Sens. Environ. 114 (10), 2160–2181.
Du, Z., et al., 2014. Analysis of Landsat-8 OLI imagery for land surface water mapping. Remote Sens. Lett. 5 (7), 672–681.
Duan, Z., Bastiaanssen, W., 2013. Estimating water volume variations in lakes and reservoirs from four operational satellite altimetry databases and satellite imagery data. Remote Sens. Environ. 134, 403–416.
Ehalt Macedo, H., Beighley, R.E., David, C.H., Reager, J.T., 2019. Using GRACE in a streamflow recession to determine drainable water storage in the Mississippi River basin. Hydrol. Earth Syst. Sci. 23 (8).
Erler, A.R., et al., 2019. Simulating climate change impacts on surface water resources within a lake-affected region using regional climate projections. Water Resour. Res. 55 (1), 130–155.
Feng, M., Sexton, J.O., Channan, S., Townshend, J.R., 2016. A global, high-resolution (30-m) inland water body dataset for 2000: First results of a topographic–spectral classification algorithm. Int. J. Digital Earth 9 (2), 113–133.
Frappart, F., Calmant, S., Cauhopé, M., Seyler, F., Cazenave, A., 2006. Preliminary results of ENVISAT RA-2-derived water levels validation over the Amazon basin. Remote Sens. Environ. 100 (2), 252–264.
Gronewold, A.D., Stow, C.A., 2014. Unprecedented seasonal water level dynamics on one of the Earth's largest lakes. Bull. Am. Meteorol. Soc. 95 (1), 15–17.
Hamlington, B., Reager, J., Chandanpurkar, H., Kim, K.Y., 2019. Amplitude modulation of seasonal variability in terrestrial water storage. Geophys. Res. Lett. 46 (8), 4404–4412.
Hirschi, M., Seneviratne, S.I., Schär, C., 2006. Seasonal variations in terrestrial water storage for major midlatitude river basins. J. Hydrometeorol. 7 (1), 39–60.
Johnston, B.R., Hiwasaki, L., Klaver, I.J., Castillo, A.R., Strang, V., 2011. Water, cultural diversity, and global environmental change: Emerging trends, sustainable futures? Springer Science & Business Media.
Khandelwal, A., et al., 2017. An approach for global monitoring of surface water extent variations in reservoirs using MODIS data. Remote Sens. Environ. 202, 113–128.
Kottek, M., Grieser, J., Beck, C., Rudolf, B., Rubel, F., 2006. World map of the Köppen-Geiger climate classification updated. Meteorol. Z. 15 (3), 259–263.
Lu, S., Ouyang, N., Wu, B., Wei, Y., Tesemma, Z., 2013. Lake water volume calculation with time series remote-sensing images. Int. J. Remote Sens. 34 (22), 7962–7973.
Mehdinia, A., Dehbandi, R., Hamzehpour, A., Rahnama, R., 2020. Identification of microplastics in the sediments of southern coasts of the Caspian Sea, north of Iran. Environ. Pollut. 258, 113738.
Messager, M., Lehner, B., Grill, G., Nedeva, I., Schmitt, O., 2016. Estimating the volume and age of water stored in global lakes using a geo-statistical approach. Nature communications 7 (1), 1–11.
Pan, M., et al., 2012. Multisource estimation of long-term terrestrial water budget for major global river basins. J. Clim. 25 (9), 3191–3206.
Pekel, J.-F., Cottam, A., Gorelick, N., Belward, A.S., 2016. High-resolution mapping of global surface water and its long-term changes. Nature 540 (7633), 418–422.
Pekel, J.-F., et al., 2014. A near real-time water surface detection method based on HSV transformation of MODIS multi-spectral time series data. Remote Sens. Environ. 140, 704–716.
Schwatke, C., Dettmering, D., Börgens, E., Bosch, W., 2015a. Potential of SARAL/AltiKa for inland water applications. Mar. Geod. 38 (sup1), 626–643.
Schwatke, C., Dettmering, D., Bosch, W., Seitz, F., 2015b. DAHITI–an innovative approach for estimating water level time series over inland waters using multi-mission satellite altimetry. Hydrol. Earth Syst. Sci. 19 (10), 4345–4364.
Sheffield, J., Ferguson, C.R., Troy, T.J., Wood, E.F., McCabe, M.F., 2009. Closing the terrestrial water budget from satellite remote sensing. Geophys. Res. Lett. 36 (7).
Sheng, Y., et al., 2016. Representative lake water extent mapping at continental scales using multi-temporal Landsat-8 imagery. Remote Sens. Environ. 185, 129–141.
Sterling, S.M., Ducharne, A., Polcher, J., 2013. The impact of global land-cover change on the terrestrial water cycle. Nat. Clim. Change 3 (4), 385–390.
Zhu, J., Song, C., Wang, J., Ke, L., 2020. China's inland water dynamics: The significance of water body types. Proc. Nat. Acad. Sci. 117 (25), 13876–13878.
Taube, C., 2000. Three Methods for Computing the Volume of a Lake. In J. C. Schneider (Ed.). Manual of Fisheries Survey Methods II: With Periodic Updates. Michigan Department of Natural Resources, Fisheries Special Report (Chap. 12, Vol. 25, pp. 175–179). Ann Arbor.
Verpoorter, C., Kutser, T., Seekell, D.A., Tranvik, L.J., 2014. A global inventory of lakes based on high-resolution satellite imagery. Geophys. Res. Lett. 41 (18), 6396–6402.
Villadsen, H., Andersen, O.B., Stenseng, L., Nielsen, K., Knudsen, P., 2015. CryoSat-2 altimetry for river level monitoring – Evaluation in the Ganges-Brahmaputra River basin. Remote Sens. Environ. 168, 80–89.
Wada, Y., Wisser, D., Bierkens, M.F., 2014. Global modeling of withdrawal, allocation and consumptive use of surface water and groundwater resources. Earth Syst. Dyn. Discuss. 5 (1), 15–40.
Wang, J., et al., 2018. Recent global decline in endorheic basin water storages. Nat. Geosci. 11 (12), 926–932.
Williamson, C.E., Saros, J.E., Vincent, W.F., Smol, J.P., 2009. Lakes and reservoirs as sentinels, integrators, and regulators of climate change. Limnol. Oceanogr. 54 (6part2), 2273–2282.
Yang, K., et al., 2017. Recent dynamics of alpine lakes on the endorheic Changtang Plateau from multi-mission satellite data. J. Hydrol. 552, 633–645.
Yao, F., et al., 2015. High-resolution mapping of urban surface water using ZY-3 multi-spectral imagery. Remote Sens. 7 (9), 12336–12355.
Yao, F., Wang, J., Wang, C., Crétaux, J.-F., 2019. Constructing long-term high-frequency time series of global lake and reservoir areas using Landsat imagery. Remote Sens. Environ. 232, 111210.
Yeh, P.J.F., Famiglietti, J., 2008. Regional terrestrial water storage change and evapotranspiration from terrestrial and atmospheric water balance computations. J. Geophys. Res.: Atmos. 113 (D9).
Zarfl, C., Lumsdon, A.E., Berlekamp, J., Tydecks, L., Tockner, K., 2015. A global boom in hydropower dam construction. Aquat. Sci. 77 (1), 161–170.
Zawadzki, L., Ablain, M., 2016. Accuracy of the mean sea level continuous record with future altimetric missions: Jason-3 vs. Sentinel-3a. Ocean Sci. 12 (1).
Zhang, B., et al., 2011. Estimation and trend detection of water storage at Nam Co Lake, central Tibetan Plateau. J. Hydrol. 405 (1–2), 161–170.
Zhang, G., Chen, W., Xie, H., 2019. Tibetan Plateau's lake level and volume changes from NASA's ICESat/ICESat-2 and Landsat Missions. Geophys. Res. Lett. 46 (22), 13107–13118.
Zheng, J., Ke, C.-Q., Shao, Z., Li, F., 2016. Monitoring changes in the water volume of Hulun Lake by integrating satellite altimetry data and Landsat images between 1992 and 2010. J. Appl. Remote Sens. 10 (1), 016029.
Zhou, T., Nijssen, B., Gao, H., Lettenmaier, D.P., 2016. The contribution of reservoirs to global land surface water storage variations. J. Hydrometeorol. 17 (1), 309–325.